Chloride Ion Hydration and Diffusion in Supercritical Water Using a Polarizable Water Model

Masahito Kubo,[†] Ronald M. Levy,*[,‡] Peter J. Rossky,[§] Nobuyuki Matubayasi,[||] and Masaru Nakahara*[,||]

Department of Chemistry and Chemical Biology, Rutgers, The State University of New Jersey, Piscataway, New Jersey 08854-8087, Institute for Theoretical Chemistry, Department of Chemistry and Biochemistry, University of Texas at Austin, Austin, Texas 78712, and Institute for Chemical Research, Kyoto University, Uji, Kyoto 611-0011, Japan

Received: October 8, 2001; In Final Form: February 11, 2002

Chloride ion solvation in supercritical water is investigated by computer simulations, including water polarizability explicitly. Comparisons are made between the TIP4P fluctuating charge and the original TIP4P models. Particular attention is paid to the density dependence of the equilibrium structural and transport properties. The chloride ion hydration number slowly decreases with density reduction in a similar way for both the fluctuating charge and the fixed-charge water models. The diffusion coefficients for the two models also exhibit a similar density dependence, except at the lowest density examined (0.05 g/cm^3), where the chloride ion diffusion rate in polarizable water is significantly larger than that in nonpolarizable water because of a more rapid loss of the hydration shell in polarizable water at the lowest density. The remarkable similarity between the two models is related to the insensitivity of the local polarization in the first hydration shell to the bulk conditions. The results also suggest that the local viscosity rather than the long-range dielectric friction dominates the transport properties.

1. Introduction

Most common chemical and biological processes that involve solvation occur at or near room temperature and atmospheric pressure. In recent years, however, there has been increasing interest in supercritical fluid solutions. The supercritical condition is a physical state of a material above the critical point where the distinction disappears between gas and liquid. As a result, the material possesses both the diffusivity of a gas and many solvation properties of a liquid, and there have been many industrial and environmental applications using supercritical fluid solvation.[1−4] Supercritical CO_2, for instance, has been utilized for the decaffeination process of coffee.[5] In particular, supercritical water is of great interest because of its wide availability and nontoxic nature as a solvent. As an example, supercritical water provides a totally different reaction environment for toxic waste, enhancing these chemical reactions that would not occur at normal conditions and leading to nontoxic chemical products.[6,7] Therefore, studies of the physical chemistry of supercritical water are of great practical interest.

In this article, we investigate the hydration of a single chloride ion under supercritical conditions by molecular dynamics (MD) simulations using a polarizable water model, and we examine how the inclusion of the explicit polarizability influences the hydration of the chloride ion under these extreme conditions. In particular, the density dependence of various structural and transport properties is investigated over a wide range of densities. Previously, aqueous supercritical solutions including chloride ion solution have been investigated by computer simulation, primarily using nonpolarizable models.[8−14] As simplified yet powerful tools, nonpolarizable models are usually parametrized to reproduce many structural, thermodynamic, and dynamic properties in the liquid phase at ambient conditions. Under extreme conditions, supercritical or subcritical, these models are also applied to supplement often difficult experimental observations with increasing success.[8−14] Because nonpolarizable models have fixed partial charges, they have the same dipole moment at ambient or at any supercritical state. It is well-known that the average polarity of a water molecule is strongly enhanced in ambient liquid water compared to that in the gas phase because of interactions with neighbors.[10] In supercritical water, where hydrogen bonds are weaker and the water structure is less ordered, however, there is good reason to question the use of state-independent variables for the study of the density dependence of supercritical solutions, particularly at lower densities.[15]

Polarizable models are designed to reproduce the microscopic fluctuations in the polarization occurring in the real system. Polarizable models can therefore mimic the environment at each unique state, which one expects to be different from the ambient conditions most nonpolarizable models are designed to reproduce. The "correct" representation of each state may be important, given that the supercritical solution changes from the liquidlike state at higher densities to the gaslike state at lower densities along an isotherm. Recently, Koneshan et al. reported a computational study of ionic hydration using a polarizable model at a single supercritical state.[16] In that article, the difference between the nonpolarizable and the polarizable models was found to be surprisingly small, even for the diffusion coefficients. Here, we focus on a comparison between polarizable and nonpolarizable solvent models over a very large range of supercritical fluid densities.

* Corresponding authors. E-mail: ronlevy@lutece.rutgers.edu.
[†] Current address: Institute for Chemical Research, Kyoto University.
[‡] Rutgers, The State University of New Jersey.
[§] University of Texas at Austin.
[||] Institute for Chemical Research, Kyoto University.

10.1021/jp013743v CCC: $22.00
Published on Web 03/22/2002

To separate the effects of polarization fluctuations from the effects due to any average parameter differences between models, simulations using the polarizable model are compared with those using two nonpolarizable models: one is the original nonpolarizable TIP4P model, and the other is a nonpolarizable model with parameters adjusted to the average properties of the polarizable model in the bulk. Details of the models are explained in the next section. If there are differences between the explicitly polarizable model and the fixed-charge model adjusted to the average polarization at each density, they are expected to be more prominent near the solute because of the enhanced dipole moment and large polarization in the vicinity of the ion relative to that of the bulk.

The ion diffusion coefficients are influenced both by the average solvent polarization and the fluctuations in the polarization. The Stokes−Einstein law expresses the mobility of nonionic species in terms of viscous friction. Water mobility is expected to follow the trend predicted by the Stokes−Einstein law in the high-density region and then gradually approach simple kinetic theory at lower densities.[17,18] Regarding ion mobility, the Hubbard−Onsager continuum dielectric friction theory[19,20] predicts a monotonic increase as the density decreases.[21,22] Hubbard−Onsager theory is based on an electrohydrodynamic continuum model that takes both dielectric friction and viscous friction effects into account. Recent experimental and computational studies, on the contrary, show that the ion mobility reaches a maximum in the medium density region then decreases slightly toward the lower solvent density region down to about 0.2 g/cm.[3,11,21,23−26] Therefore, the limitation of the Hubbard−Onsager theory is increasingly evident toward the lower density region, despite a predicted increase in the relative contribution of dielectric friction. As the fluidity of water continuously increases with the density decrease, on the other hand, there should be a point where the ion mobility eventually begins to increase. Few studies, however, have investigated this low-density region, except the recent study by Hyun et al.,[27] because of experimental diffuculties. Thus, the trend of ion dynamics is not well established beyond the appearance of a plateau in the medium-density region. We expand our investigation to the very low density region and see that a further increase in ion mobility is indeed present.

2. Methods

In this section, we first briefly describe the polarizable model used in this study. More details of the fluctuating charge model can be found in the original articles by Berne and coworkers.[28,29] Simulation details are presented in the following subsection.

2.1. Fluctuating Charge Model. In the fluctuating charge model (fluc-*q*),[28] the partial charge on each atomic site fluctuates in response to its surrounding. The distribution of the partial charges at every configuration is determined by solving a self-consistent equation given by the electronegativity equalization principle.[30] The fluc-*q* model differs from other induced dipole models[31−39] in two important respects. First, it has polarizabilities to all orders in the electric moments. Second, it is computationally efficient because the more common dipole−dipole interaction is replaced in the fluc-*q* by modified Coulomb amplitudes, which increases the computational effort by only a factor of 1.1 according to Rick et al.[28]

As a polarizable water model, we adopted a fluc-*q* version of the TIP4P model, TIP4P-FQ.[40,28] This water model was successfully used for the study of chloride ion solvation at ambient conditions.[29] It should be noted, however, that the Lennard−Jones (LJ) parameters are different from those of the original TIP4P modeled by Jorgensen et al. to reproduce accurate liquid properties at ambient conditions:[40,28] σ is slightly increased from 3.154 to 3.159 Å whereas ϵ is nearly doubled from 0.155 to 0.2862 kcal/mol. Combining the changes in both σ and ϵ, the LJ potential is slightly steeper and narrower at the minimum. The molecular geometry is the same as that for the TIP4P model. Intermolecular charge transfer is not allowed in our study.

The chloride ion is nonpolarizable in this study. It bears a constant unit negative charge. The OPLS model[41] is used for the LJ potentials, where the heteroatomic interactions are given by the geometric mean rules. The ion−water interaction is thus modeled with the combination of fixed LJ potential and electrostatic interaction due to the charge fluctuation on the water molecules. The fact that this chloride ion model is specifically parametrized for TIP4P water makes the choice of our water models appropriate. However, the combination of TIP4P water and OPLS chloride ion tends to overestimate the hydration number at ambient conditions.[29] It should also be noted that both the TIP4P and TIP4P-FQ models apparently exhibit a significantly lower critical temperature ($T_c \approx 575$ K) compared to that of real water ($T_c = 647$ K.)[42−44]

2.2. Simulation Procedures. The MD simulations are performed in the following manner. A single nonpolarizable chloride ion is placed in a cubic box that contains 256 water molecules, with periodic boundary conditions and the minimum image convention.[45] The Ewald summation is implemented to handle the electrostatic potentials. A molecular cutoff based on the oxygen−oxygen distance is applied at $L/2$ to the real space portion of all pair interactions, where L is the length of the unit simulation box. The screening parameter is set to $5/L$, and 256 reciprocal lattice vectors are used. Simulations are carried out at constant volume at each density. For integration of the equations of motion, we use a time-reversible molecular dynamics algorithm for rigid bodies in the quaternion representation recently developed by Dullweber et al. and subsequently and independently by us.[46,47] This algorithm allowed us to use a 2 fs time step with good energy conservation.

As it is a polarizable model, the partial charges on TIP4P-FQ water fluctuate in response to the configuration of the surrounding environment. The solvent partial charge distribution, determined using an extended equation of motion by adding fictitious "masses" to the charges, is solved for iteratively in each configuration until the electronegativity at each atomic site in a molecule becomes equal.

Two nonpolarizable water models are considered: one is the original TIP4P water model, and the other is a nonpolarizable TIP4P-like water model (called TIP4P-m hereafter) that involves the same average bulk dipole moment as does TIP4P-FQ for each simulation condition. TIP4P-m has the same LJ parameters as does the TIP4P-FQ model. The static partial charges of TIP4P-m are modified from those of the original TIP4P to represent the "correct" average dipole moment at each thermodynamic condition. In practice, the dipole moment is determined from the polarizable simulations with TIP4P-FQ and a chloride ion from the average dipole moment of water molecules at the farthest separation from the ion. The dipole moments obtained are 2.32, 2.14, 2.06, 1.97, 1.92, and 1.89 D for solvent densities of 1.0, 0.6, 0.4, 0.2, 0.1, and 0.05 g/cm^3, respectively, at 400 °C. The TIP4P-FQ dipole moment at ambient conditions is 2.62 D. Comparing the polarizable model with the TIP4P-m model, the effect of the charge fluctuation, aside from the average shift of the dipole moment, is directly seen in a clearer way than it

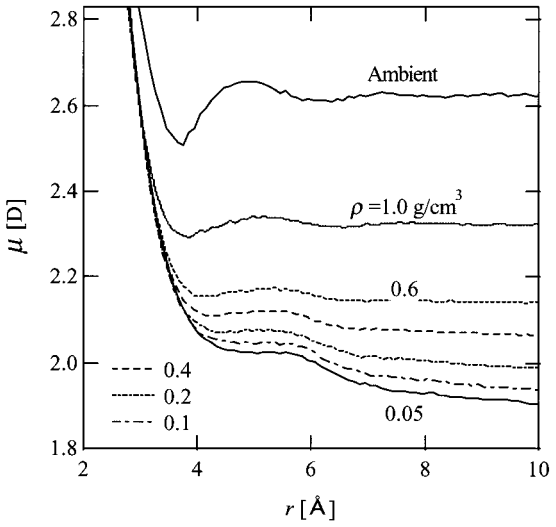

Figure 1. Local dipole moment at different densities (g/cm^3). Except for ambient, the temperature is 400 °C.

is with the original TIP4P model, which has a fixed dipole moment of 2.18 D. This information is particularly important for the current study with varying densities because some equilibrium properties could well be sensitive to the average dipole moment of water at a given density and temperature.[15] In all models, the water geometry is fixed at the TIP4P structure.

Each simulation is run for 1.1 ns with a 2 fs time step, except at 0.05 g/cm^3. Because of the large statistical uncertainty associated with the TIP4P-FQ or TIP4P-m model results at the density of 0.05 g/cm^3, the simulations were extended to 2 ns at this density. For error analyses that are particularly important for the diffusion calculations, the samples are averaged over blocks of 100 ps each.

3. Results and Discussion

3.1. Radial Structure. The first and foremost quantity of interest for the polarizable model is the dipole moment distribution. Figure 1 shows the average local dipole moment of the TIP4P-FQ water as a function of the distance from the chloride ion. Interestingly, there is little density dependence near the solute ($r \leq 3.5$ Å) at 400 °C, although the values are not as large as the values for ambient conditions. The dipole moment falls sharply to a value close to the bulk value (by 4 Å) from the solute and then shows a small, broad peak between 5 and 6 Å. The clear first minimum and the second peak, which are distinctive characteristics of the ambient solution, are faint at best for all the supercritical states. At densities of 0.6 g/cm^3 and below, the bulk dipole moment values are smaller than that of nonpolarizable TIP4P. It should be noted that having a dynamically adjustable dipole moment is significant only very near the solute, where the strong ion−water interaction is dominant, although there is some effect at longer distances at very low density. Roughly speaking, beyond 4 Å, the bulk density is the primary factor that determines the local dipole moment.

The radial structure of water around the solute is commonly described in terms of the radial distribution function. The radial distribution function, however, is not well-suited for comparison of the radial structure around the solute at different supercritical densities because of the differences in the bulk density values. Instead, we consider the local density distribution $\rho(r)$, which is defined as the product of the bulk density and the solute−solvent radial distribution function.

The height of the first peak remains relatively constant over the density range of 0.6−0.2 g/cm^3, particularly with TIP4P (Figure 2). At the much higher density (1.0 g/cm^3), the peak is steeper, though not as steep as at ambient conditions. When the density is 0.1 g/cm^3 or less, on the other hand, there is a relatively rapid decline in the height of the peak. The polarizable model exhibits a sharper decline at very low density, suggesting a more rapid breakage of water clustering around the ion. The density dependence of the height of the first peak is similar to that from other computational results[12] with the SPC/E water model[48] at a reduced temperature of 1.05. On the other hand, the results with TIP4P-m show a monotonic decrease in the first peak as the density decreases, corresponding to the gradual decrease in the average dipole moment. As a result, the height of the peak is smaller than those of the other two models; at ambient conditions, it is comparable to TIP4P.

Another characteristic of the radial structure is the location of the first and second peaks. The first peak remains approximately at the Cl−O distance of 3.2 Å from the solute for both ambient and all supercritical conditions, indicating the dominant effect of the direct interaction between the solute and the closest solvent. In contrast, the second peak becomes virtually invisible for lower density supercritical solutions and increases from the ambient position from less than 5 to greater than 6 Å, which suggests that the rigidity of the many-body hydrogen bond network of water around the ionic solute rapidly disappears for supercritical solutions at lower densities, although there remain strong nearest-neighbor interactions.

3.2. Hydration Numbers. The hydration number is calculated by integrating the local density distribution up to a given fixed cutoff value. Results are summarized in Table 1. They show generally similar trends compared to those from the results reported from a previous computational study with the nonpolarizable SPC/E model[11] using integration to the first minimum in the density destribution. All models show a gradual decrease in the hydration number with decreasing density. Though commonly reported and treated as one of the leading indices of solvation structure, we note that the hydration number is a somewhat ambiguous indicator that depends on the definition of the hydration shell, particularly in the present case. Balbuena et al., for instance, previously reported nearly equal hydration numbers for chloride ion solution at ambient and at several supercritical conditions on the basis of simulations using the SPC/E model.[9] These values were based on a fixed cutoff radius of 4.75 Å for supercritical solutions and 4.00 Å for ambient. However, because a hydration shell expansion trend is observed here with a density decrease at 400 °C, the validity of keeping the same cutoff radius for all supercritical conditions is arguable. Therefore, at least two types of shell cutoffs could be defined: the first involves fixing the cutoff radius for all the densities, such as Balbuena et al. did, regardless of the character of the water structure around the solute and the other involves integrating the local density to the point where it reaches the first minimum. However, the cutoff defined by the second method is difficult to implement unambiguously because the first minimum becomes increasingly vague as the density decreases, as is evident in Fig 2.

With a fixed cutoff of 4.75 Å for supercritical solutions, our results show a clear density dependence (Figure 3(a)). There is a fairly monotonic decline in the hydration number with both polarizable and nonpolarizable models. Although this result does not agree with the finding of ref 9 that suggested little change in the hydration number at ambient and a broad range of supercritical conditions, this difference may be due to simulation

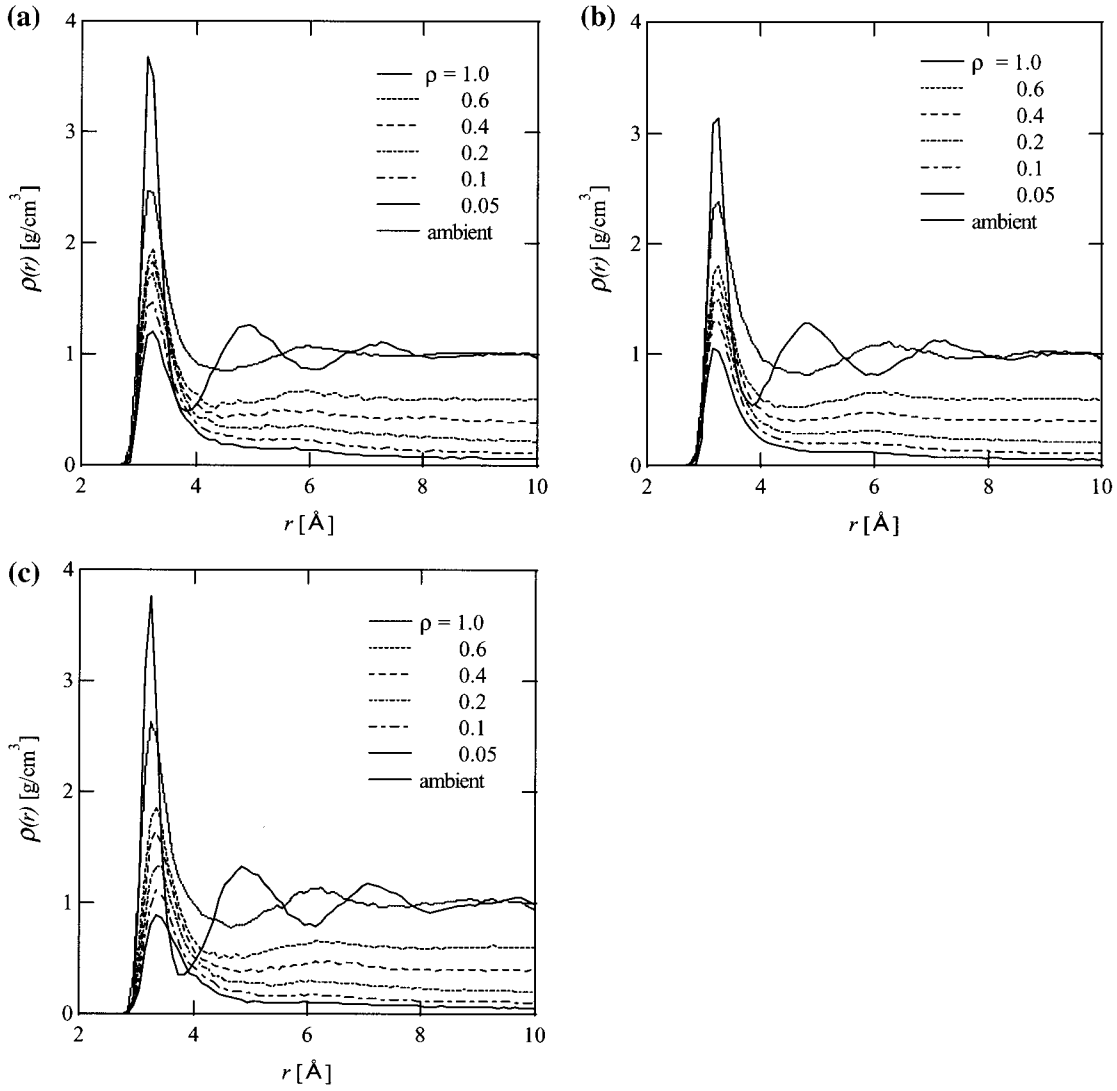

Figure 2. Comparison of local density profiles among different densities (g/cm^3) for (a) TIP4P, (b) TIP4P-FQ, and (c) TIP4P-m.

conditions and the models. In particular, as mentioned in the previous section, both the TIP4P and the TIP4P-FQ models apparently exhibit a significantly lower T_c than does the SPC/E model.[42,44,49] The effective simulation temperature is therefore higher in our study by about 10%. It is known that for SPC/E, a higher temperature results in a greater density dependence of the hydration number.[9,50]

Balbuena et al. attributed the small change in the hydration number to the much stronger ion−water interactions compared to the strength of the water−water interactions.[9] From our results, the very strong ion−water interactions appear to be important for chloride supercritical solutions as far away from the solute as the location of the first density peak (∼3.2 Å). Up to this distance, the local dipole moment is virtually unchanged over a large range of densities (Figure 1). Beyond the first maximum, however, there is a clearer density dependence, as seen in the local density. The effect is most notable beyond the first shell in the disappearance of the second peak in the local density. Thus, the local density approaches the bulk value quickly beyond the first maximum. The hydration number is an integral value of the local density from the solute to the cutoff radius, and the outer solvent density is increasingly weighted by the factor r^2. As a result, the hydration number we compute with the fixed cutoff radius is expected to have some density dependence.

Because we chose a cutoff at the first minimum for the calculation of the hydration number, on the other hand, our results suggest that there is a plateau roughly between 0.2 and 0.6 g/cm^3, which is particularly evident with the TIP4P model (Figure 3b). The plateau is less evident with the TIP4P-FQ model. At the highest density (1.0 g/cm^3), the hydration number of TIP4P-FQ is greater than that of TIP4P. A sharp decline is clearly present for densities below 0.2 g/cm^3, in correspondence with the trend of the local density at very low densities. The appearance of the plateau at medium densities can be understood as a compensation between the local density decline and the hydration shell expansion. The fact that the hydration shell expansion is more rapid with TIP4P (4.40−4.80 Å) than with TIP4P-FQ (4.55 to 4.85 Å in Table 1), combined with a smaller decrease in the first peak, explains the more evident plateau for TIP4P. The hydration shell expansion, however, introduces a complexity in the analysis of the hydration number. Even if the number of water molecules within the hydration shell remains fairly constant at medium densities, water molecules within the shell may behave differently depending on their variable proximity to the ion at each condition. Measuring the distance profile of the residence time of water within the hydration shell may reveal dynamic differences at different densities that cannot be distinguished with the hydration number alone. This issue will be the subject of a future study.

TABLE 1: Number of Water Molecules around the Chloride Ion

model	ρ (g/cm^3)	T (K)	r (Å)	n_{ClO}	model	ρ (g/cm^3)	T (K)	r (Å)	n_{ClO}
TIP4P	1.0	298	3.85[a]	7.3	TIP4P-FQ			4.65[a]	7.6
			4.00	7.8				4.75	8.0
TIP4P-FQ			3.85[a]	6.5	TIP4P-m[b]			4.65	7.9
			4.00	7.1				4.75	8.3
TIP4P-m[b]			3.85	6.5	SPC/E, ref 11[d]				7.5
			4.00	6.9	TIP4P	0.2	673	4.75	7.9
SPC/E, ref 9			4.0	7.4				4.80[a]	8.0
TIP4P, ref 38			3.85[c]	7.4	TIP4P-FQ			4.75	6.7
TIP4P	1.0	673	4.45[a]	11.6				4.85[a]	7.0
			4.75	13.9	TIP4P-m[b]			4.75	6.9
TIP4P-FQ			4.65[a]	13.1				4.85	7.2
			4.75	13.9	SPC/E, ref 9	0.29		4.75	8.1
TIP4P-m[b]			4.65	13.2	SPC/E, ref 11[d]	0.22			6.8
			4.75	13.9	TIP4P	0.1	673	4.75	6.6
TIP4P	0.6	673	4.40[a]	8.1				5.0[a]	7.1
			4.75	9.8	TIP4P-FQ			4.75	5.6
TIP4P-FQ			4.55[a]	8.3				4.9[a]	5.9
			4.75	9.3	TIP4P-m[b]			4.75	5.6
TIP4P-m[b]			4.55	8.6				4.9	5.8
			4.75	9.6	SPC/E, ref 9	0.087		4.75	7.5
SPC/E, ref 11[d]	0.61			8.3	TIP4P	0.05	673	4.75	5.3
TIP4P	0.4	673	4.50[a]	7.8				5.2[a]	6.1
			4.75	8.8	TIP4P-FQ			4.75	4.4
								5.2[a]	5.0
					TIP4P-m[b]			4.75	4.5
								5.2	5.0

[a] The cutoff radius r is set where the first minimum is located. Values are given in multiples of 0.05 Å for the density of 0.2 and above and in multiples of 0.1 Å for the density below 0.2. [b] The cutoff radius is the same as for TIP4P-FQ for the same density. Dipole moments are 2.32, 2.14, 2.06, 1.97, 1.92, and 1.89 D for densities of 1.0, 0.6, 0.4, 0.2, 0.1, and 0.05 g/cm^3, respectively. The dipole moment for ambient is 2.62 D. [c] The cutoff is an approximation. [d] The upper cutoff radii are not provided but are stated to correspond to the first minimum.

It is also interesting to note that at lower densities the polarizable model exhibits a somewhat smaller hydration number than does the TIP4P model, which is probably due to the smaller TIP4P-FQ dipole moment at these lower densities relative to the fixed TIP4P dipole moment, except for contact with the ion. Thus, the increased dipole moment of TIP4P-FQ near the ion relative to that of TIP4P appears to have a smaller effect at these lower densities. However, the comparison between TIP4P and TIP4P-FQ models is not straightforward because the LJ parameters are also different. The fact that the results with TIP4P-m model (see Table 1) are in excellent agreement with the TIP4P-FQ model reveals that the slight overestimation of the hydration numbers with TIP4P in comparison with those of TIP4P-FQ is due to the significant deviation between the average dipole moments far from the ion rather than a fingerprint of the explicit polarizability.

3.3. Diffusion Coefficients. Regarding the transport properties, we consider here the diffusion coefficient computed from the mean square displacement. Our result for water diffusion D_{H_2O} shows excellent agreement with available experimental results[17] as well as qualitative agreement with the results reported by Yoshii et al.[18] The water mobility increases dramatically as the density decreases (Figure 4). This result is expected because as the solvent becomes less dense the translational motion of a water molecule should be closer to free motion. At lower densities, the water diffusion process is described by simple kinetic theory rather than by the hydrodynamic Stokes−Einstein law.[51,17] Although in general the polarizable results show slightly larger mobility, they are nonetheless qualitatively similar.

The ion diffusion D_{Cl^-} shows a very different density dependence from that of D_{H_2O} (Table 2, Figure 5). Although in general the ion diffusion increases as the density decreases, the rate is far slower than that of water diffusion. When the density decreases from 1.0 to 0.2 g/cm^3, the ion mobility increases only by 2.5-fold whereas D_{H_2O} increases by over 8-fold. Hubbard−Onsager theory has been used to analyze these transport coefficients. As reported in the analysis by Ibuki et al.,[22] Hubbard−Onsager theory is qualitatively applicable only in the high-density and high-pressure region, where the molecular packing effects and long-range dielectric friction seen in other high-density liquids are more effective.[21] We note that a molecular theory based on the interaction site model for the dynamics of ions in polar liquids in this regime has recently been presented.[52]

In the medium-density region between 0.6 and 0.4 g/cm^3, D_{Cl^-} reaches a plateau; there is only a slight change in the ion mobility for both the TIP4P and TIP4P-FQ solvent models. This finding is qualitatively consistent with other recent computational studies using the SPC/E water model,[11,23,27] as well as experimental and theoretical analyses.[21,22,24−26,] The quantitative differences between Cl^- diffusion coefficients in SPC/E water reported in refs 11 and 27 and listed in Table 2 may be due to differences in the ion−water potential employed and the treatment of the long-range electrostatic interactions. Studies suggest that the ion mobility may have a small local maximum in the 0.3−0.45 g/cm^3 range[53] then decrease slightly with further density reduction. Our results, strictly speaking, do not show such a trend other than a slight decrease well within the error from 0.6 to 0.4 g/cm^3 with the TIP4P-FQ model. It should be noted, however, that the errors associated with experimental measurements are increasingly large for the lower densities where supercritical water has a low dielectric constant because the dissociation constant of a salt decreases dramatically at such low densities. Thus, quantitative comparisons with the experimental data are often difficult to make. Even so, compared with the solvent mobility, the appearance of a plateau at intermediate densities is a unique characteristic of ion mobility in supercritical water solution.[22]

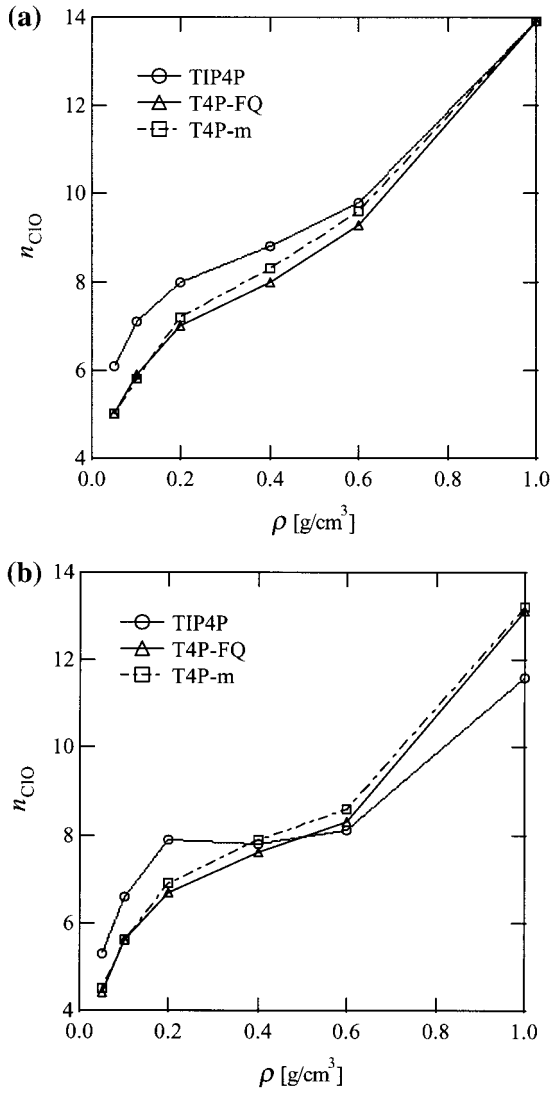

Figure 3. Comparison of the hydration numbers as defined with (a) a fixed cutoff radius of 4.75 Å for all supercritical conditions and (b) a different cutoff for each condition. Errors are within 0.1.

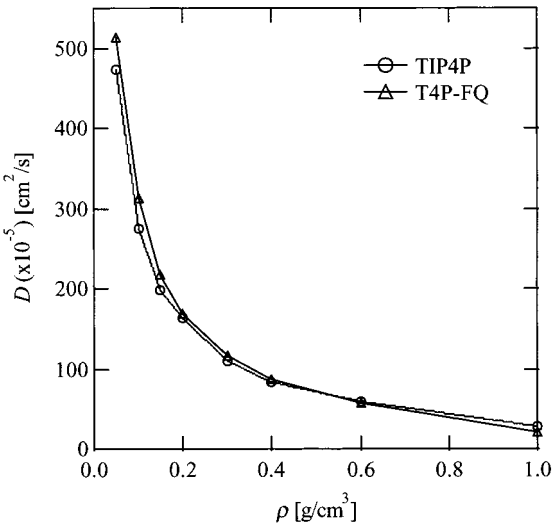

Figure 4. Comparison of the diffusion coefficient of water among different densities. The simulation length is 200 ps. Errors are within 3% of the *D* values.

After reaching the plateau, our results show a steep rise in mobility at densities of 0.2 g/cm^3 and below, particularly with the TIP4P-FQ model. This finding parallels the results for the local density and the hydration number, again suggesting the rapid breakdown of the structure around the ion in the very low density range. A similar increase has also been observed for Cl^- in SPC/E water.[27] The results with TIP4P-m, which has a dipole moment value identical to that of TIP4P-FQ in the bulk, show nearly identical diffusion coefficients D_{Cl^-} to those from the TIP4P results. At the lowest density, 0.05 g/cm^3, the TIP4P and TIP4P-m models have dipole moments that differ by about 15%, and the TIP4P-FQ dipole moment in the first hydration shell (see Figure 1) is comparable to that of TIP4P (2.18 D). On the other hand, D_{Cl^-} for the TIP4P-FQ model is 50% larger than the corresponding values in TIP4P and TIP4P-m solvent. Hence, the enhanced increase in ion mobility for the polarizable solvent model is not readily assigned to average dipole moments per se. The fact that the rate of the hydration shell breakage with the density decrease is not correlated obviously to local or bulk dipole moments suggests that the charge asymmetry and dipole moment fluctuations within the individual solvent molecules, present only with the polarizable model, contribute to the enhanced ion dynamics. It would be interesting to study this issue further.

Except at the lowest densities, ionic diffusion values in the polarizable and nonpolarizable solvent models show excellent agreement with each other, both qualitatively and quantitatively. This quite remarkable result is evident as well in the structural analysis discussed earlier, although the agreement of the diffusion constants among the models is perhaps even closer. The first hydration shells are structurally very similar among the models over the intermediate density range. However, the dipole moments are quite different at longer distance, hence the dielectric friction exerted on the ions by the more distant solvent is expected to be very different. This finding suggests that the similarity in the ion diffusion constants in polarizable and nonpolarizable solvent as well as the slow variation in mobility in the intermediate density regime reflects the dominant frictional contribution from the solvent close to the ion. These short-range ion−solvent effects on transport in the low and intermediate density supercritical fluid regime are not repre-

TABLE 2: Diffusion Coefficients of the Chloride Ion at 400 °C ($\times$ 10^{-5} cm^2/S)

ρ (g/cm^3)	TIP4P	TIP4P-FQ	TIP4P-m	SPC/E	HO[a]	exptl[b]
1.0	17.8 ± 2.6	18.1 ± 2.4	18.0 ± 3.0	23 ± 2[c]		
0.8				20.7[d]	33.2	31.8
0.74				33.4 ± 3.1[e]		
0.61				38.8 ± 4.2[e]		
0.6	37.7 ± 5.2	38.7 ± 5.1	33.7 ± 5.3		40.5	37.3
0.5				29.2[d]	43.9	39.6
0.48				41.7 ± 5.5[e]		
0.4	37.9 ± 5.9	35.1 ± 4.3	39.0 ± 5.5	43.5 ± 5.9[e]	47.2	41.5
0.31				44.1 ± 5.0[e]		
0.3					50.8	41.1
0.29				29.2[d]		
0.22				42.1 ± 3.5[e]		
0.2	48.7 ± 6.9	50.4 ± 7.9	42.7 ± 5.8	43.5 ± 5.9[e]	54.9	
				40 ± 5[c]		
0.15				34.9[d]		
0.1	59.0 ± 8.9	62.7 ± 9.3	59.8 ± 9.2			
0.087				48.1[d]		
0.05	81 ± 10	123 ± 24	83 ± 25			

[a] Hubbard-Onsager theory, ref 22. [b] Experimental values are reported in ref 22. Errors are stated to be increasingly large at lower densities. [c] SPC/E model, ref 14. Simulations were performed at 410 °C. [d] SPC/E model, ref 27. Values were interpreted from the figure in the reference. Errors are roughly 10% of the diffusion values. [e] SPC/E model, ref 11.

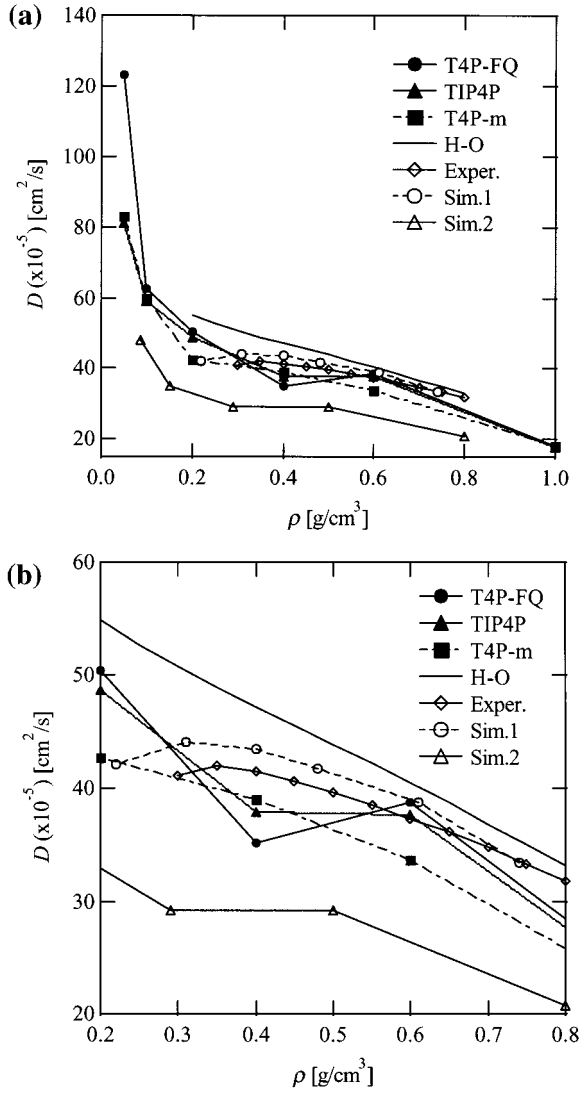

Figure 5. Comparison of the chloride ion diffusion coefficient (a) at different densities and for (b) magnification at medium density. The total simulation length is greater than 2000 ps at $\rho = 0.05$ g/cm^3 for TIP4P-FQ and TIP4P-m. All other simulation lengths are 1100−1500 ps. For the experiment (ref 22) and HO theory (ref 22), diffusion coefficients are reported as 50% of those for NaCl. Our simulation results, simulation 1 (ref 11) and simulation 2 (ref 27), correspond to the chloride ion diffusion coefficient calculated directly.

sented well in a uniform density continuum theory like the Hubbard−Onsager model. We note, however, that at densities from 0.3 to about 0.1 g/cm^3 a large decrease in mobility due to electrostriction beyond the first solvation shell is predicted by the compressible continuum model.[54] At lower densities, this long-range electrostriction is still present in the compressible continuum model, but it no longer decreases the mobility because the viscosity of the water is essentially independent of density at low densities.

4. Conclusions

We have investigated the equilibrium structural and transport properties of chloride ion solvated in supercritical water using the polarizable TIP4P-FQ water model and two comparable nonpolarizable models. Despite the added complexity of the state dependence in the dipole and higher multipole moments, the differences in the investigated properties are, most notably, strikingly small. This result is consistent with the conclusion of another recent study using a different polarizable water model.[16] There are quantitative differences, particularly at the lowest densities where the polarizable model manifests a more rapid loss of the hydration shell with decreasing density. Some small quantitative differences, such as in the hydration number, can be attributed to the reduced dipole moment of the polarizable model at lower densities. In that case, TIP4P-m that reproduces the bulk dipole moment obtained with the polarizable model shows better agreement than does the TIP4P model. In other cases, however, the difference in the dipole moment does not explain the difference between the polarizable and nonpolarizable models. In particular, the diffusion coefficient at the very lowest density obtained with the TIP4P-m model is close to the value in TIP4P water despite the significantly reduced dipole moment in the bulk relative to that in TIP4P. This result suggests that explicit dipole moment fluctuations of first shell solvent molecules have a significant effect on the transport at the lowest density studied. Further investigations are needed to clarify the mechanism.

Many properties investigated in this study show a parallel dependence on density for polarizable and nonpolarizable models. In the higher-density region ($\rho > 0.6$ g/cm^3), where packing effects keep molecules close together, the density dependence is clearly evident. The diffusive behavior of the chloride ion can be described in this high-density region by the Hubbard−Onsager theory,[22] which takes the hydrodynamic continuum effects of dielectric friction and viscous friction into account. In the medium-density region (0.2−0.6 g/cm^3), however, the density dependence is weak. When the density becomes gaslike, the state is no longer hydrodynamic and binary collisions should apply, although a small hydration shell around the ion is still present, even at a bulk density value as small as 0.05 g/cm^3. Hubbard−Onsager theory does not describe ionic diffusion in supercritical water at low and intermediate densities very well. One approach that is being pursued to model the transport behavior in this regime is the introduction of a compressible continuum model for which the parameters are distance-dependent.[54,27] Further experimental and computational investigations are needed to establish a more comprehensive theoretical description of transport over the very wide range of solvent densities encountered in supercritical fluids.

Acknowledgment. The Rutgers and Kyoto groups are supported by a joint JSPS-NSF award for travel MPCR-395/98-15256 and NSF INT-9815256. We acknowledge partial support for this work from the Columbia University Center for Biomolecular Simulations (NIH P41 RR06892). P.J.R. is grateful to the R.A. Welch Foundation for support of this work. M.N. is grateful to the Research Grant-in-Aid from the Ministry of Education, Science, and Culture (No. 10304047 and 13440179). N.M. is grateful to the Research Grant-in-Aid from the Ministry of Education, Science, and Culture (No. 11740322 and 13640509). The Japan group is also supported by the CREST (Core Research for Evolutional Science and Technology) of Japan Science and Technology Corporation (JST). We thank Dr. Anders Wallqvist for his assistance in the early stages of this study.

References and Notes

(1) Spiess, F. N. et al. *Science* **1980**, *207*, 1421.
(2) Shaw, R. W.; Brill, T. B.; Clifford, A. A.; Eckert, C. A.; Franck, E. U. *Chem. Eng. News* **1991**, *69*, 26.
(3) Seewald, J. S. *Nature (London)* **1994**, *370*, 285.
(4) Nakahara, M.; Yamaguchi, T.; Ohtaki, H. *Recent Res. Dev. Phys. Chem.* **1997**, *1*, 17.
(5) McHugh, M.; Krukonis, V. *Supercritical Fluid Extraction*, 2nd ed.; Butterworth-Heinemann: Stoneham, MA, 1994.

(6) Savage, P. E. *Chem. Rev.* **1999**, *99*, 603.
(7) Yamasaki, Y.; Enomoto, H.; Yamasaki, N.; Nakahara, M. *Bull. Chem. Soc. Jpn.* **2000**, *73*, 2687.
(8) Chialvo, A. A.; Cummings, P. T. *J. Phys. Chem.* **1996**, *100*, 1309.
(9) Balbuena, P. B.; Johnston, K. P.; Rossky, P. J. *J. Phys. Chem.* **1996**, *100*, 2706.
(10) Balbuena, P. B.; Johnston, K. P.; Rossky, P. J.; Hyun, J.-K. *J. Phys. Chem. B* **1998**, *102*, 3806.
(11) Lee, S. H.; Cummings, P. T.; Simonson, J. M.; Mesmer, R. E. *Chem. Phys. Lett.* **1998**, *293*, 289.
(12) Chialvo, A. A.; Cummings, P. T.; Simonson, J. M.; Mesmer, R. E. *J. Chem. Phys.* **1999**, *110*, 1064.
(13) Rasaiah, J. C.; Noworyta, J. P.; Koneshan, S. *J. Am. Chem. Soc.* **2000**, *122*, 11182.
(14) Noworyta, J. P.; Koneshan, S.; Rasaiah, J. C. *J. Am. Chem. Soc.* **2000**, *122*, 11194.
(15) Matubayasi, N.; Wakai, C.; Nakahara, M. *J. Chem. Phys.* **1999**, *110*, 8000.
(16) Koneshan, S.; Rasaiah, J. C.; Dang, L. X. *J. Chem. Phys.* **2001**, *114*, 7544.
(17) Lamb, W. J.; Hoffman, G. A.; Jonas, J. *J. Chem. Phys.* **1981**, *74*, 6875.
(18) Yoshii, N.; Yoshie, H.; Miura, S.; Okazaki, S. *J. Chem. Phys.* **1998**, *109*, 4873.
(19) Hubbard, J.; Onsager, L. *J. Chem. Phys.* **1977**, *67*, 4850.
(20) Hubbard, J. *J. Chem. Phys.* **1978**, *68*, 1649.
(21) Ibuki, K.; Ueno, M.; Nakahara, M. *J. Phys. Chem. B* **2000**, *104*, 5139.
(22) Ibuki, K.; Ueno, M.; Nakahara, M. *J. Mol. Liq.*, in press.
(23) Lee, S. H.; Cummings, P. T. *J. Chem. Phys.* **2000**, *112*, 864.
(24) Gruszkiewicz, M. S.; Wood, R. H. *J. Phys. Chem. B* **1997**, *101*, 6549.
(25) Ho, P. C.; Palmer, D. A. *Geochim. Cosmochim. Acta* **1997**, *61*, 3027.
(26) Ho, P. C.; Palmer, D. A. *J. Chem. Eng. Data* **1998**, *43*, 162.
(27) Hyun, J.-K.; Rossky, P. J.; Johnston, K. P. *J. Phys. Chem. B* **2001**, *105*, 9302.
(28) Rick, S. W.; Stuart, S. J.; Berne, B. J. *J. Chem. Phys.* **1994**, *101*, 6141.
(29) Stuart, S. J.; Berne, B. J. *J. Phys. Chem.* **1996**, *100*, 11934.
(30) Sanderson, R. T. *Science* **1951**, *114*, 670.
(31) Stillinger, F. H.; David, C. W. *J. Chem. Phys.* **1978**, *69*, 1473.
(32) Barnes, P.; Finney, J. L.; Nicholas, J. D.; Quinn, J. E. *Nature (London)* **1979**, *282*, 459.
(33) Rullman, J. A. C.; van Duijnen, P. T. *Mol. Phys.* **1988**, *63*, 451.
(34) Sprik, M.; Klein, M. L. *J. Chem. Phys.* **1988**, *89*, 7556.
(35) Ahlström, P.; Wallqvist, A.; Engström, S.; Jönsson, B. *Mol. Phys.* **1989**, *68*, 563.
(36) Cieplak, P.; Kollman, P.; Lybrand, T. *J. Chem. Phys.* **1990**, *92*, 6755.
(37) Dang, L. X. *J. Chem. Phys.* **1992**, *97*, 2659.
(38) Wallqvist, A.; Berne, B. J. *J. Phys. Chem.* **1993**, *97*, 841.
(39) Bernardo, D. N.; Ding, Y.; Krogh-Jespersen, K.; Levy, R. M. *J. Phys. Chem.* **1995**, *98*, 4180.
(40) Jorgensen, W.; Chandrasekhar, J.; Madura, J.; Impey, R.; Klein, M. *J. Chem. Phys.* **1983**, *79*, 926.
(41) Chandrasekhar, J.; Spellmeyer, D.; Jorgensen, W. *J. Am. Chem. Soc.* **1984**, *106*, 903.
(42) Liew, C. C.; Inomata, H.; Arai, K. *Fluid Phase Equilib.* **1998**, *144*, 287.
(43) Vorholz, J.; Harismiadis, V. I.; Rumpf, B.; Panagiotopoulos, A. Z.; Maurer, G. *Fluid Phase Equilib.* **2000**, *170*, 203.
(44) Yoshii, N.; Miyauchi, R.; Miura, S.; Okazaki, S. *Chem. Phys. Lett.* **2000**, *317*, 414.
(45) Allen, M.; Tildesley, D. *Computer Simulation of Liquids;* Oxford University Press: New York, 1993.
(46) Dullweber, A.; Leimkuhler, B.; McLachlan, R. *J. Chem. Phys.* **1997**, *107*, 5840.
(47) Matubayasi, N.; Nakahara, M. *J. Chem. Phys.* **1999**, *110*, 3291.
(48) Berendsen, H.; Grigera, J.; Straatsma, T. *J. Phys. Chem.* **1987**, *91*, 6269.
(49) Guissani, Y.; Guillot, B. *J. Chem. Phys.* **1993**, *98*, 8221.
(50) Flanagin, L. W.; Balbuena, P. B.; Johnston, K. P.; Rossky, P. J. *J. Phys. Chem. B* **1997**, *101*, 7998.
(51) Hausser, R.; Maier, G.; Noack, F. *Z. Naturforsch., A: Phys. Sci.* **1966**, *21*, 1410.
(52) Chong, S.-H.; Hirata, F. *J. Chem. Phys.* **1999**, *111*, 3654.
(53) The ion mobilities are reported in terms of molar conductance in such studies.
(54) Xiao, C.; Wood, R. H. *J. Phys. Chem. B* **2000**, *104*, 918.